

Flattening modulus of a neutron star by rotation and magnetic field

K. Konno, T. Obata, and Y. Kojima

Department of Physics, Hiroshima University, Higashi-Hiroshima 739-8526, Japan

Received

Abstract. We calculated the ellipticity of the deformed star due to the rotation or magnetic field. These two effects are compared to each other within general relativity. It turned out that the magnetic distortion is important for recently observed candidates of magnetars, while the magnetic effect can be neglected for well-known typical pulsars.

Key words: relativity – stars: neutron – stars: rotation – stars: magnetic fields – methods: analytical

1. Introduction

Observations of pulsars have been accumulated since the first discovery by Hewish et al. (1968), and several new types of pulsars appeared with great surprise. These observations have partially revealed the structure and evolution of rotating neutron stars. Their rotation periods range from 1.5 ms to several seconds. The surface magnetic fields range from 10^8 to 10^{15} G. The upper limit was recently raised by a factor 10^3 by the discovery of the soft gamma-ray repeaters (SGRs) and anomalous X-ray pulsars (AXPs) (see e.g. Kouveliotou et al. 1998, 1999; Mereghetti & Stella 1995). The new class of pulsars with the very strong magnetic field ($B \sim 10^{14}$ – 10^{15} G) are most likely candidates of *magnetars* (e.g. Thompson & Duncan 1996) and may be worth studying further. In the future, we may find a more extreme case, that is, a rapidly rotating relativistic star with a strong magnetic field.

Most stars have spherically symmetric structure. They are however deformed due to the rapid rotation and the strong magnetic field. It is well known that both effects produce a flattening equilibrium star. We will examine them within general relativity. These effects are assumed to be small and treated as perturbations to spherically symmetric stars. The rotational axis of pulsars does not in general coincide with the axis of the dipole magnetic

field. The relativistic treatments for the case is a complicated task, because the situation is not stationary. In this paper, however, we assume that the rotational effect decouples from the magnetic effect. Thus we consider the deformation arising from each perturbation separately and estimate the ellipticity. The estimate is important to judge which effect dominates in the rotating magnetized stars, whose rotation rate and the magnetic field are in a wide range. Our treatment is beyond the classical estimate in the Newtonian gravity, and give better comparison of the rotational effect and the magnetic effect on star deformation for various pulsars. When either of them is huge, our estimate breaks down, and sophisticated numerical codes are required (see e.g. Bocquet et al. 1995; Bonazzola & Gourgoulhon 1996).

The paper is organized as follows. In Sect. 2, we briefly review deformation of stars due to the rotation (Chandrasekhar 1933; Chandrasekhar & Roberts 1963) and the magnetic field (Chandrasekhar & Fermi 1953; Ferraro 1954; Gal'tsov et al. 1984; Gal'tsov & Tsvetkov 1984) within Newtonian gravity. The quadrupole deformation can be evaluated by the ellipticity of the equilibrium shape. In Sect. 3, we also calculate the ellipticity based on the general relativistic perturbation theory (see also Hartle (1967) and Chandrasekhar & Miller (1974) for the rotational cases and Konno et al. (1999) for the magnetic cases). The ellipticity can be summarized in the same form as the Newtonian cases, but with different numerical factors. In Sect. 4, using the ellipticity, we compare the rotational effect with the magnetic effect on star deformation numerically. In this comparison, we keep the parameter range of known pulsars in mind. Finally, we give concluding remarks in Sect. 5. Throughout the paper, we use the units in which $c = G = 1$.

2. Simple estimate of deformation

Quadrupole deformation of an equilibrium body is characterized by the ellipticity ε , which is defined by

$$\varepsilon = \frac{\text{equatorial radius} - \text{polar radius}}{\text{mean radius}}. \quad (1)$$

For the gravitational equilibrium with uniform rotation, the value is essentially related to the ratio of the rotational energy to the gravitational energy. In the slow rotation of a homogeneous star, we have a well-known result (see e.g. Chandrasekhar 1969):

$$\varepsilon_{\Omega} = \frac{5}{4} \frac{R^3 \Omega^2}{M}, \quad (2)$$

where R , M and Ω denote the radius, mass and angular velocity, respectively. For other stellar model, the numerical factor $5/4$ should be replaced by an appropriate one. For example, the factor is 0.76 for the model with the polytropic equation of state (EOS) $p = \kappa \rho^{(n+1)/n}$ with index $n = 1$ (see Table 1 in Chandrasekhar & Roberts 1963). We therefore generalize the expression with a dimensionless factor f as

$$\varepsilon_{\Omega} = f \frac{R^3 \Omega^2}{M}, \quad (3)$$

and will discuss how the factor f depends on the stellar models.

In a similar way, the effect of the magnetic stress is also expressed by the energy ratio of the magnetic field to the gravitational field. Introducing a dimensionless factor g , we have the ellipticity ε_B arising from magnetic field as

$$\varepsilon_B = g \frac{\mu^2}{M^2 R^2}, \quad (4)$$

where μ is the magnetic dipole moment. The dimensionless factor g , in general, depends on both the magnetic field configurations and the EOS. For example, in the case of an incompressible fluid body with a dipole magnetic field treated by Ferraro (1954), we derive $g = 25/2$.

3. Relativistic calculation of deformation

In this section, we will review quadrupole deformation due to the slow rotation and weak dipole magnetic field. The deformation can be expressed by the second-order quantities with respect to the rotation rate or the magnetic field strength. In order to calculate the shape, we also have to calculate the space-time metric, which is axisymmetric stationary or static one. The line element can be written in the form

$$\begin{aligned} ds^2 = & -e^{\nu(r)} [1 + 2\{h_0(r) + h_2(r)P_2(\cos\theta)\}] dt^2 \\ & + e^{\lambda(r)} \left[1 + \frac{2e^{\lambda(r)}}{r} \{m_0(r) + m_2(r)P_2(\cos\theta)\} \right] dr^2 \\ & + r^2 (1 + 2k_2(r)P_2(\cos\theta)) \\ & \times [d\theta^2 + r^2 \sin^2\theta (d\phi - \omega(r)dt)^2], \end{aligned} \quad (5)$$

where P_2 is the Legendre's polynomial of degree 2, and $(h_0, h_2, m_0, m_2, k_2)$ are the second-order quantities for the rotation rate or the magnetic field strength. The quantity

ω is the angular velocity acquired by an observer falling freely from infinity to a point r , and is equal to zero for the static magnetic field deformation.

The stress-energy tensor of the perfect fluid body is described by

$$T_{(m)}^{\mu}_{\nu} = (\rho + p) u^{\mu} u_{\nu} + p \delta^{\mu}_{\nu}. \quad (6)$$

When we consider the magnetic field deformation, we further take into account the stress-energy tensor arising from the magnetic field, i.e.,

$$T_{(em)}^{\mu}_{\nu} = \frac{1}{4\pi} \left(F^{\mu\lambda} F_{\nu\lambda} - \frac{1}{4} F_{\sigma\lambda} F^{\sigma\lambda} \delta^{\mu}_{\nu} \right). \quad (7)$$

Solving the Einstein-Maxwell equations, we can obtain the second-order metric functions mentioned above.

The ellipticity of the relativistic star can be calculated from the definition (1) as

$$\varepsilon = -\frac{3}{2} \left(\frac{\xi_2}{r} + k_2 \right), \quad (8)$$

where ξ_2 represents the displacement of quadrupole deformation.

Since the displacement of the surface can be determined by the hydrostatic equilibrium condition, the ellipticity of the slowly rotating star is expressed as (Chandrasekhar & Miller 1974)

$$\varepsilon_{\Omega} = \frac{3}{r\nu'} h_2 + \frac{r}{\nu'} e^{-\nu} (\Omega - \omega)^2 - \frac{3}{2} k_2. \quad (9)$$

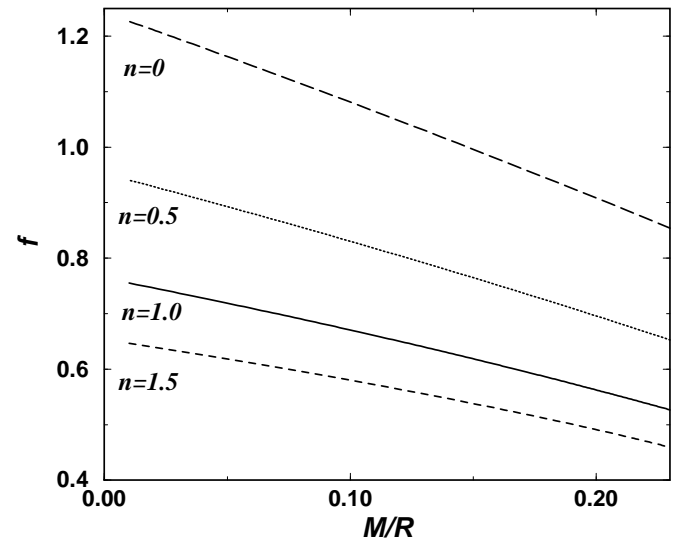


Fig. 1. The dimensionless factor f , that is, the ellipticity of the rotational cases normalized by $R^3 \Omega^2 / M$, which is plotted against M/R .

In order to compare it with the Newtonian results, we normalize the ellipticity in the same form as Eq. (3). There

are several possibilities of the normalization factors for M and R in the relativistic calculation. We use natural choices, i.e., gravitational mass for M and circumferential radius for R in this paper. This normalization is useful to extrapolate from the Newtonian results. Chandrasekhar & Miller (1974) used a different normalization, which causes a prominent peak (see Fig. 5 in their paper). We note that the peak is due merely to a less convenient choice of the normalization. The resultant dimensionless factor f is calculated for the polytropic EOS with $n = 0, 0.5, 1, 1.5$. Fig. 1 displays the variation of the dimensionless quantity f with respect to the relativistic factor M/R . This figure shows that the correct relativistic calculations give smaller values of the ellipticity than those of the Newtonian calculations with fixed $R^3\Omega^2/M$. The factor in the typical relativistic case decreases down to 0.7 of the Newtonian case.

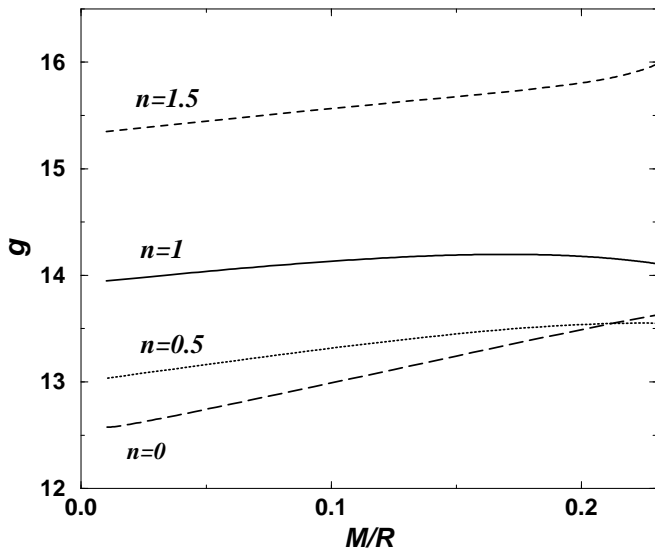


Fig. 2. The dimensionless factor g , that is, the ellipticity of the magnetic case normalized by $\mu^2/(M^2R^2)$, which is plotted against M/R . (Note that the normalization of this figure is different from that of Konno et al. (1999).)

As for the weakly magnetized star, the Lorentz force plays a role on the equilibrium. The rotational term $\Omega - \omega$ is replaced by the magnetic term in the ellipticity. From the hydrostatic condition, we have (Konno et al. 1999)

$$\varepsilon_B = \frac{3}{r\nu'}h_2 + \frac{2r}{\nu'(\rho_0 + p_0)}J^\phi A^\phi - \frac{3}{2}k_2, \quad (10)$$

where the subscript ‘0’ denotes the background quantities, and J^ϕ and A^ϕ are the ϕ -components of the 4-current and 4-potential respectively. The ellipticity can also be written in the form of Eq. (4). We also use the gravitational mass M and circumferential radius R . Fig. 2 displays the

variation of the ellipticity with respect to the relativistic factor M/R . In these calculations, we have used the current distribution

$$J^\phi \propto \rho_0 + p_0, \quad (11)$$

which is a simplest case derived by the integrability condition (see e.g. Ferraro 1954) and gives the direct general-relativistic extension of Ferraro (1954). Using the normalization, the residual factor g is almost independent of the relativistic factor M/R .

4. The comparison

In order to compare the rotational effect with the magnetic effect on star deformation, we now consider the ratio of ε_Ω to ε_B ,

$$\frac{\varepsilon_\Omega}{\varepsilon_B} = \frac{f}{g} \left(\frac{R^3\Omega^2}{M} \right) \left(\frac{\mu^2}{M^2R^2} \right)^{-1}. \quad (12)$$

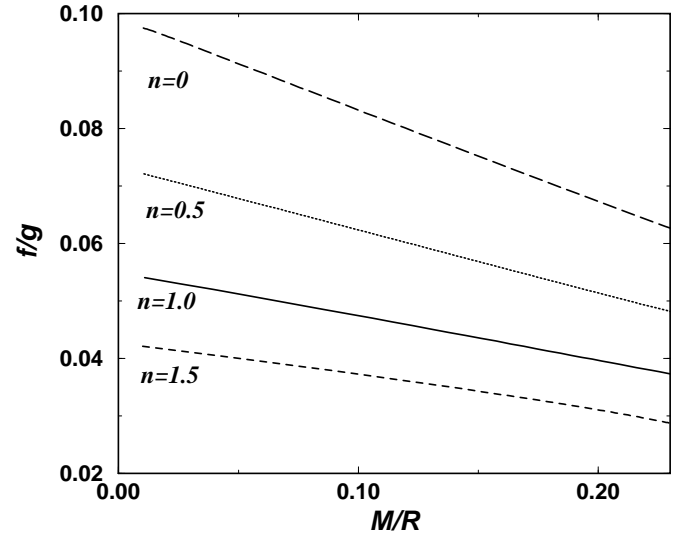


Fig. 3. The ratio of the two dimensionless factors, f/g , plotted against M/R .

First, we investigate the dependence of the ratio of the two dimensionless factors, f/g , on the relativistic factor M/R . Fig. 3 displays this ratio. From this figure, we can see that the true relativistic calculations with $M/R \sim 0.2$ give smaller values of the ratio than those obtained by the Newtonian calculations. This fact means that the approach using the Newtonian gravity overestimates the rotational effect. The curves f/g are approximately reproduced within 10% if we use

$$\frac{f}{g} \approx \frac{1 - 1.4M/R}{10 + 8n}. \quad (13)$$

Next, we consider the comparison including other parameters Ω and μ of stars. We use the stellar model with $M = 1.4M_\odot$ and $R = 10\text{km}$. Fig. 4 displays a critical line on which $\varepsilon_\Omega = \varepsilon_B$ and the two regions divided by this line in B - Ω space, where B denotes the typical magnetic field strength on the surface, which is defined by $B = \mu/R^3$. We have plotted only one representative line of $n = 1$. We can also derive very close results for other indices. The critical line, in general, can be written from Eq. (12) as

$$B[\text{G}] \approx 5.3 \times 10^{13} \sqrt{\frac{f}{g}} \left(\frac{M/1.4M_\odot}{R/10\text{km}} \right)^{1/2} \Omega [\text{sec}^{-1}], \quad (14)$$

where it is useful to use the fitting formula Eq. (13) for f/g . In the region I, the magnetic effect dominates the rotational effect, i.e., $\varepsilon_B > \varepsilon_\Omega$, whereas in the region II vice versa, i.e., $\varepsilon_\Omega > \varepsilon_B$. From this figure, we find that objects having magnetic field strength $B \sim 10^{14}$ – 10^{15}G and period $T \sim 1$ sec such as SGRs and AXPs belong to the region I. Thus, the magnetic effect overwhelms the rotational effect for such observed candidates of magnetars. On the other hand, well-known typical pulsars with

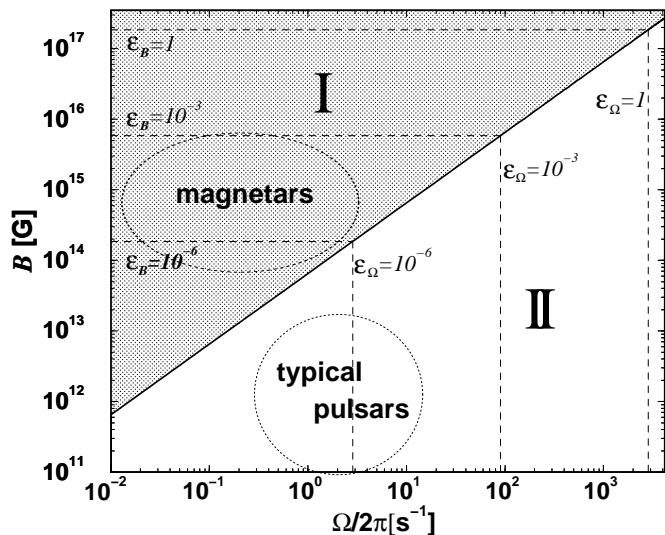


Fig. 4. The critical line on which $\varepsilon_\Omega = \varepsilon_B$ in B - Ω space for $M/R = 0.2$. This line divides the B - Ω space into two regions. In the region I, the magnetic effect dominates the rotational effect, while in the region II vice versa.

magnetic field strength $B \sim 10^{11}$ – 10^{13}G and the period $T \sim 10^{-1}$ – 1 sec (see e.g. Taylor et al. 1993) obviously belong to the region II. Millisecond pulsars also belong to the region II. The magnetic deformation is neglected.

5. Concluding remarks

The new classes of objects, which are candidates of magnetars, have inspired us to investigate the relation between

the rotational effect and the magnetic effect on deformation of stars. We have briefly reviewed the quadrupole deformation due to the rotation and that due to the magnetic field based on previous studies, and compared the rotational effect with the magnetic effect for various pulsars reported observationally. From our investigation, we have found that the new classes of objects such as SGRs and AXPs belong to the region in which the magnetic effect dominates the rotational effect, while well-known typical pulsars with magnetic field strength 10^{11} – 10^{13}G and millisecond pulsars vice versa. Thus, the critical line on which the ellipticity arising from the rotation equals to that arising from the magnetic field divides the new classes and the well-known pulsars. Once we obtain the parameters Ω , B , R and M of a pulsar, we can see whether the magnetic effect is dominant or the rotational effect is dominant using Eqs. (13) and (14) and Fig. 4. The deformation due to the magnetic field may come into play in the spin-down of the magnetars. The spin-down history of the AXPs is rather irregular. Recently, Melatos (1999) ascribed the irregularity to the radiative precession produced by the deformation. At present, the fit to the observational data is not so good, but will be improved by detailed models. Theoretical models for the deformed stars will be required there.

As discussed by Bonazzola & Gourgoulhon (1996), the non-axisymmetric distortion is also important for the gravitational emission. The deformation can be calculated from the magnetic field, which is estimated from the observed pulsar period and the period derivative. The inferred amplitudes of the gravitational waves are too small for the present known pulsars. In the future, we might find more extreme case such as the early stage of rapidly rotating magnetars.

Acknowledgements. We would like to thank Dr. A.Y. Potekhin for fruitful comments and suggestions.

References

- Bocquet M., Bonazzola S., Gourgoulhon E., Novak J., 1995, A&A 301,757
- Bonazzola S., Gourgoulhon E., 1996, A&A 312,675
- Chandrasekhar S., 1933, MNRAS 93, 539
- Chandrasekhar S., 1969, Ellipsoidal Figures of Equilibrium, Yale University Press, New Haven
- Chandrasekhar S., Fermi E., 1953, ApJ, 118, 116
- Chandrasekhar S., Miller J. C., 1974, MNRAS 167, 63
- Chandrasekhar S., Roberts P. H., 1963, ApJ, 138, 801
- Ferraro V. C. A., 1954, ApJ, 119, 407
- Gal'tsov D. V., Tsvetkov V. P., 1984, Phys. Lett. 103A, 193
- Gal'tsov D. V., Tsvetkov V. P., Tsurulev A. N., 1984, Zh. Eksp. Teor. Fiz. 86, 809; Sov. Phys. JETP 59, 472
- Hartle J. B., 1967, ApJ 150, 1005
- Hewish A., et al., 1968, Nat 217, 709
- Konno K., Obata T., Kojima Y., 1999, A&A 352, 211
- Kouveliotou C., et al., 1998, Nat 393, 235
- Kouveliotou C., et al., 1999, ApJ 510, L115

Melatos A., 1999, ApJ 519, L77

Mereghetti S., Stella L, 1995, ApJ 442, L17

Taylor J. H., Manchester R. N. and Lyne A. G., 1993 ApJ
Suppl., 88, 529

Thompson C., Duncan R. C., 1996, ApJ 473, 322